

SENSOR FUSION FOR HYDROGRAPHIC MAPPING APPLICATIONS

L. Estep

J. Lillycrop

L. Parson

U.S. Army Engineer Waterways Experiment Station
Coastal Engineering Research Center
3909 Halls Ferry Road
Vicksburg, MS 39180

BIOGRAPHICAL SKETCH

Dr. Lee Estep has been with CERC for a year and a half. He has been a member of the SHOALS team during this period. A primary goal of his work is the coupling of the SHOALS LIDAR with airborne passive scanner data to further enhance the SHOALS environmental dataset. Prior to coming to CERC, Dr. Estep worked with the Naval Research Laboratory. There he provided expertise in ocean color remote sensing, LIDAR systems, and ocean optics. His main research interest centers on the extraction of useful environmental information from the remote sensing of coastal water areas.

Mr. Jeff Lillycrop is a Research Engineer in the Engineering Applications Unit, Coastal Structures and Evaluation Branch, Engineering Development Division at the Coastal Engineering Research Center (CERC), Waterways Experiment Station, Vicksburg, MS. He received a B.S. in engineering sciences (1981) and a M.S. in coastal and oceanographic engineering (1983) from the University of Florida. Mr. Lillycrop worked two years in the Jacksonville District's Coastal Planning Branch on a variety of erosion control and hurricane protection projects. Since joining CERC in 1986 he has been involved in many coastal studies and the development of the SHOALS system. He is currently the Program Manager of the SHOALS development program.

Mr. Larry Parson is Research Physical Scientist in the Coastal Geology Unit, Coastal Structures and Evaluation Branch, Engineering Development Division at the Coastal Engineering Research Center (CERC), Waterways Experiment Station, Vicksburg, MS. He received a B.A. in Earth Science from Millersville University of Pennsylvania (1977) and a M.S. in Oceanography from Florida Institute of Technology (1982). Prior to joining CERC, Mr. Parson worked for a private firm as a Systems Engineer providing system hardware and software design for photogrammetric applications. He joined CERC in 1991 and has been involved in monitoring coastal project performance and software design of the SHOALS system.

ABSTRACT

Bathymetric data represents valuable information to various US and International government agencies. The US Army Corps of Engineers (USACE) has recently successfully field tested the Scanning Hydrographic Operational Airborne LIDAR Survey (SHOALS) system in Sarasota, FL. The SHOALS is a state of the art Airborne LIDAR Hydrographic (ALH) system to be used by the USACE for performing bathymetric surveying in support of USACE missions. A project that merges the SHOALS system and an imaging spectrometer as a proposed, permanent dual sensor system, provides, over a survey area, both SHOALS depth information and hyperspectral imagery of the survey area. This paper focusses on the use of this dual sensor system for the bathymetric charting of coastal water areas.

INTRODUCTION

The SHOALS uses a pulsed, 200 Hz, Nd:YAG laser, which provides two different transmitted wavelengths, to sense the air-sea interface and the sea bottom. The time difference between the reception of the surface and bottom signals, corrected for angle of entry, provides an estimate of the water depth. The SHOALS is presently flown on a NOAA Bel1212 Helicopter and operates nominally, at 200 m altitude and 25 m/sec velocity. The pulse pattern on the water surface results in a uniform sounding grid with about 5 m grid spacing. Table 1 provides other information concerning the SHOALS system. For more in-depth information on the SHOALS system see Lillycrop and Banic (1992). The SHOALS provides water depth information accurate to International Hydrographic Organization (IHO) standards. However, in the near future, the SHOALS will also be capable of providing an estimate of the rate at which a light field (at the LIDAR wavelength) will decay as it transits the water column. Such information is embedded in the fall-off of the backscattered LIDAR light seen at the SHOALS receiver. The computation of the depth in the post-processing of the SHOALS survey data is enhanced if such water optical information is available on a shot-to-shot basis. The water optical information provided by SHOALS is in the form of a system attenuation coefficient, k_{sys} . This system attenuation coefficient can be related to the water optical properties of the coastal waters overflown (Gordon, 1982). In particular, k_{sys} approaches the absorption coefficient, a (Jerlov, 1976), of the water for a large receiver field of view. At the other extreme, for a very small receiver field of view, k_{sys} approaches the beam attenuation coefficient, c (Jerlov, 1976). Billard (1986) has shown how to use the results of Gordon (1982) to extract relevant water optical parameters. Using this water optical information together with the depth data, the effective optical depth of the water mass can be reckoned for each LIDAR pulse. Since little coastal water optical data is available, such information is valuable -especially on a seasonal basis.

An imaging spectrometer can be defined as providing access to several tens of spectral channels (not necessarily simultaneously) with very narrow spectral channel widths -emulating, in this wise, a laboratory spectrometer. A specific version of an imaging spectrometer is the Compact Airborne Spectrographic Imager (CASI). The CASI is rentable from several groups, both commercial and academic, and has provided researchers with reliable datasets which have been published in the remote sensing literature. The CASI is a line scanner that uses a diffraction grating to produce 288 spectral channels. The CASI can be operated in either a spectrometer mode or a spatial mode. The spectrometer mode provides for 39 'look' angles over a scene with high-resolution spectral information at 1.8 nm width. The 39 spectral look angles are overlaid on a reference image collected in a single band. The spatial mode provides for scene imagery in up to 15 channels -however the channels accessible by the CASI run from 420 nm to 900 nm at 3 nm spectral resolution. The channel selection is set in hardware and is quickly and easily changeable at the computer console. Recently, an updated version has become available that provides increased signal to noise in the blue -by 2:1. This is due to a new coating that has been placed on the grating. This means that spectral resolution attainable in the blue will be enhanced. For more detailed information see Borstad (1989).

RELATED EARLIER WORK

Lyzenga (1985) using the M8 active/passive scanner at two sites in the Bahama Islands, showed the feasibility of combining LIDAR depths with image data. The LIDAR data had to be manually interpreted for each used point. The LIDAR depths were then used to calibrate the passive image data. Then, using a band ratio technique, each band ratio was plotted against the lidar depths to see which ratio correlated best. This formed the basis of a regression derivation between the selected band ratio and depth. This regression relation was then applied to the entire image to extract depth from the information represented by the image.

The Airborne Bathymetric Survey (ASS) of the US Navy endeavored to use the Hydrographic Airborne LASER Sounder (HALS) together with the NORDA scanner (which, in effect, emulated a TM bandset) to provide depth and image data fusion (Haimbach et al., 1988). However, continual problems with the HALS and scanner caused the project to produce little useable data.

Borstad and Vosburg (1993) used LIDAR data from the Larsen 500- an operational ALH system since the mid-1980's -and CASI imagery to produce a fusion of imagery with a Digital Depth Model (DDM) based on

Larsen bathymetric data near the Bruce Peninsula in lake Huron. Although several lines of overlapping Larsen and CASI data were taken, only a relatively small subset of the data was ever processed. However, the results of this work were readily recognized by the authors as a potentially valuable environmental product.

BACKGROUND: SHOALS + CASI SARASOTA OVERFLIGHT

During the SHOALS field trials the CASI was flown over the SHOALS test flightlines. The imagery was recorded in a bandset which had 12 different wavelengths. These are provided in Table 1. This bandset

Table 1: CASI bandset used in Sarasota

BANDSET (nm)
426-470
473-501
504-527
540-569
598-621
625-656
656-667
671-684
686-690
710-714
744-760
839-869

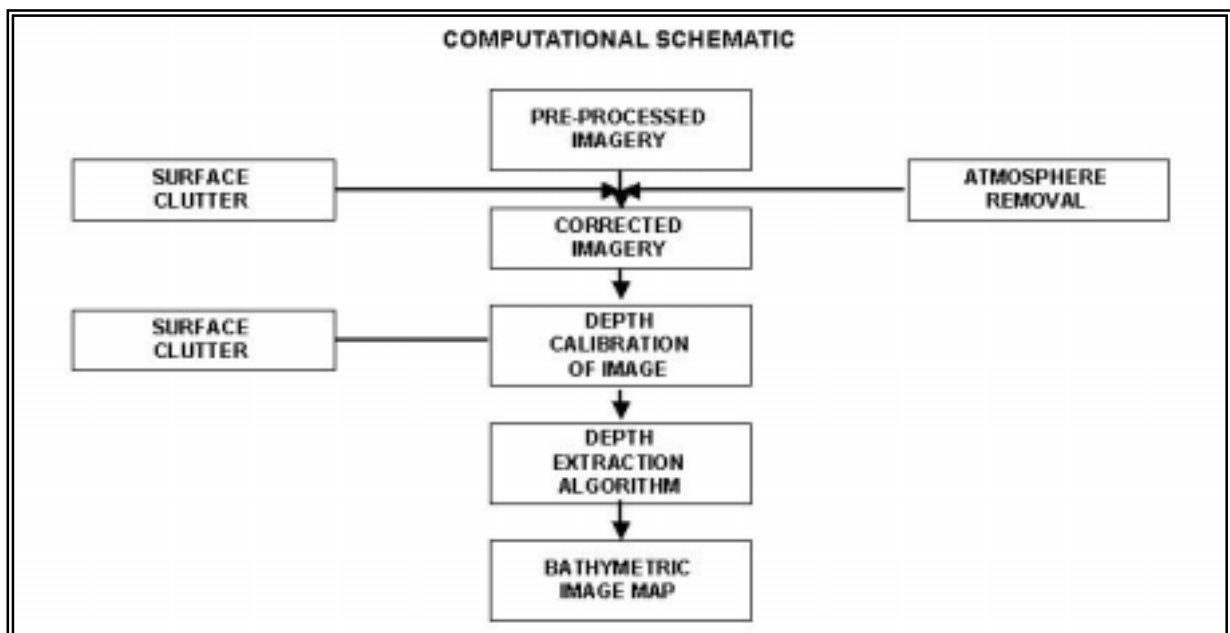
Table 1: CASI bandset emulated (with considerations for water vapor and oxygen atmospheric absorption lines and CASI SNR constraints in the blue region) NASA's proposed SeaWiFS ocean color sensor bandset. The CASI data was radiometrically corrected, roll and pitch corrected, and georeferenced using a GPS system. Thus, each pixel of a CASI image could be referenced to a particular latitude and longitude. Data were acquired at three different altitudes so that an atmospheric correction could be computed. Also, 'deep' water scenes were imaged for potential subtraction from shallow water imagery (Philpot, 1989).

The SHOALS datasets over the flightlines and benchmark areas were provided in X,V,Z format with the X and V representing latitude and longitude and Z as depth. The depth and position data were read onto a PC harddisk along with the ~ASI imagery in preparation for deriving the bathymetric image maps.

FUSING THE CASI AND SHOALS DATA

Figure 1 shows a schema that outlines the steps taken to produce bathymetric image maps. The preprocessed data block shown in Figure 1 indicates CASI image data that has already been roll, pitch, and radiometrically corrected as well as georeferenced. The atmosphere correction uses the three altitudes at

Figure 1: Computational schematic for the derivation of bathymetric image shown.



which data was collected to compute an atmospheric correction for each band under consideration. The atmospheric correction also takes into account the fact that towards the edges of the swath seen by the CASI the atmospheric slant range increases, This increase is~ corrected for in the atmospheric correction process and results in a 'flattened', atmospherically corrected Image. The surface clutter removal uses the standard approach of weighting a band in the red and subtracting it from the water penetrating bands in the blue-green region. Since light of different colors penetrate to different ~depths, with blue penetrating more and red much less, the red band sees only the topmost portion of the water ~column. The red band, when weighted appropriately, removes the surface (clutter) which is the layer of water it sees.

There are several depth extraction techniques that are readily available. We will discuss four generic approaches: 1) gridding the ~depth database, 2) correlation of spectral data to depth, 3) adaptive filter (moving window) approach, and 4) using water optical information to obtain depth from the spectral data.

Technique 1 does not use image spectral intensity information at all. That is, in the stead of the imagery helping to 'grid' the LIDAR calibration depth data through relative intensity values, a computer routine simply grids up the LIDAR depth data so that the Image array and depth array are the same size. In this case, the image serves to 'present' or 'integrate' the depth data for the user of the coastal water image map. Of course, observable bottom information and other scene information is embedded in the image presentation.

Technique 2 (Borstad and Vosburg, 1993) uses single spectral bands to correlate against depth data to see which band correlates best. One would use the band with the best correlation to derive an intensity to depth regression relation. The regression relation would then be used to compute depth over the entire image. A variant of this technique was used by Lyzenga (1985), which uses ratios of bands for the correlation computation and subsequent regression derivation. The use of ratios, it is felt, helps to offset some of the atmospheric and surface noise effect~.

Technique 3 uses an adaptive filter, or 'moving window', approach. The need for the moving window is to take into account changing water optics and bottom reflectances over a scene. Pixel intensity values are a function not only of water depth but of light attenuation and bottom reflectance (assuming atmosphere and surface effects have been dealt with). With calibration depth data available, then shifting water optics and bottom reflectance can be effectively managed by moving sequentially through the image while tying a calibrated depth to small subsetting regions. Using this kind of moving window within the image tends to minimize the non-signal (non-signal = changing bottom reflectance, changing water optics; signal = changing depth) sources of variation in light field intensity.

Technique 4 uses the fact that the light reaching the sensor is composed of light due to water column reflectance and bottom reflectance (assuming atmosphere and surface light are removed). At this point. Two different approaches can be followed: 1) compute depth based on changes in water column light - neglecting any bottom contribution to the upwelling light stream, and 2) compute depth by modeling out the influence of the water column leaving only the bottom reflectance contribution to the upwelling light stream.

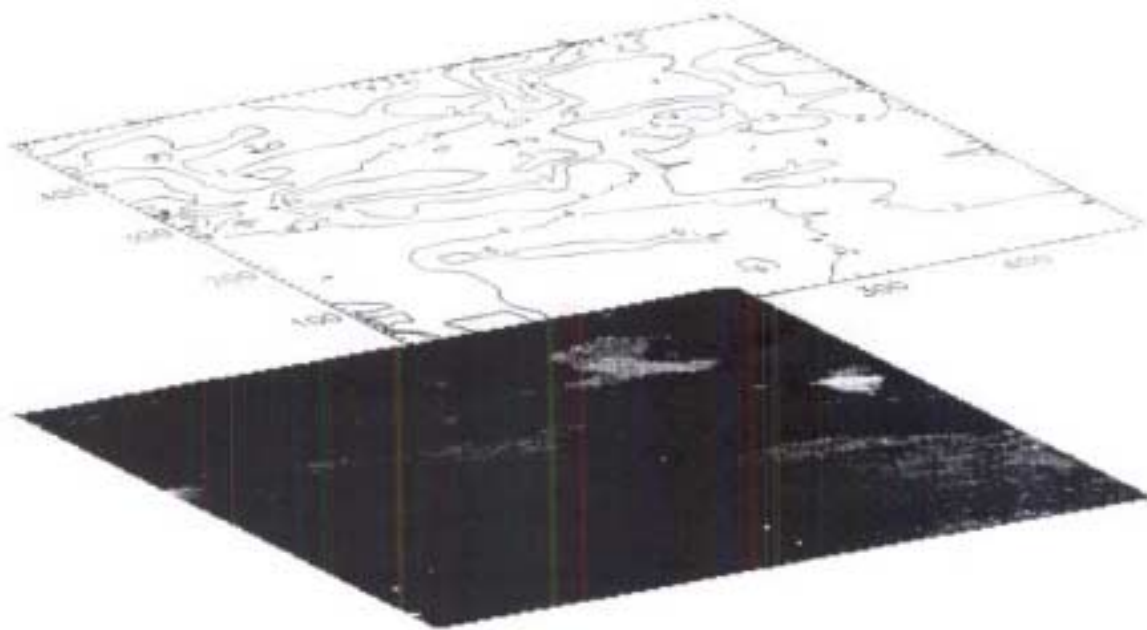
Ji et al. (1992) suggests that when the bottom reflected signal is relatively small, one ought to use water reflectance rather than bottom reflectance to estimate water depth. Use is made of a simple radiative transfer model (Philpot, 1987) to compute the water reflectance values when the presence of a bottom, at z , is felt in the upwelling light stream. However, a measure of k must be provided to enable the water depth computation.

Estep (1993) used the converse approach. The water reflectance is modeled and subtracted from the atmospherically and surface~ corrected signal seen at the sensor to leave only the signal due to the bottom light field. The absorption and backscattering values must be determined to compute the water reflectance. Once computed and subtracted from the sensor signal, the bottom component remains. The bottom reflectance, R_b , can be modeled as

$$R(\lambda, z) = R_b(\lambda) \exp(-2k_0 z)$$

(Philpot, 1987) where k_0 is an effective attenuation coefficient, and spectral R_b is the reflectance of the bottom sediment facies. In this approach, then, as in the approach of Ji et al. (1992), we still need concomitant water optical Parameters to compute the water depth.

Figure 2



RESULTS AND DISCUSSION

Figure 2 shows a stacked image of a section of Sarasota Bay; Florida. The image provides information on how the bottom type varies across the scene while the top layer of the figure shows a contour plot of depth to the nearest foot. To read the stacked plots, first locate the point of interest on the image and, then, look at the contour overlay to read the associated depth contour. The coordinate values shown are in array pixel coordinates. However, these are relatable to geographic coordinates. The depths for the contouring were computed using Technique 3 -obviating the need for water optical data while allowing for a varying bottom reflectance. The calibrated depths used with the imagery were from SHOALS depth data as well as from depth data provided locally.

Once water optical information becomes available from the SHOALS data stream, Technique 4 approaches will become feasible. At that time, a combined approach of the Ji et al. (1992) and Estep (1993) methods could be used in depth calculations. That is, when a clearly evident bottom is shown in the imagery, the Estep (1993) approach could be used. However, when the bottom is dark or not plainly visible, the Ji et al. (1992) approach would be selected.

An interesting variant of this technique would be to use the water optical information and depth information from the SHOALS to compute the diffuse optical depth at each calibrated point in the image. This would allow, upon the modeling of the water reflectance, a direct computation of the in situ spectral bottom reflectance values using Equation (1).

Figure 3

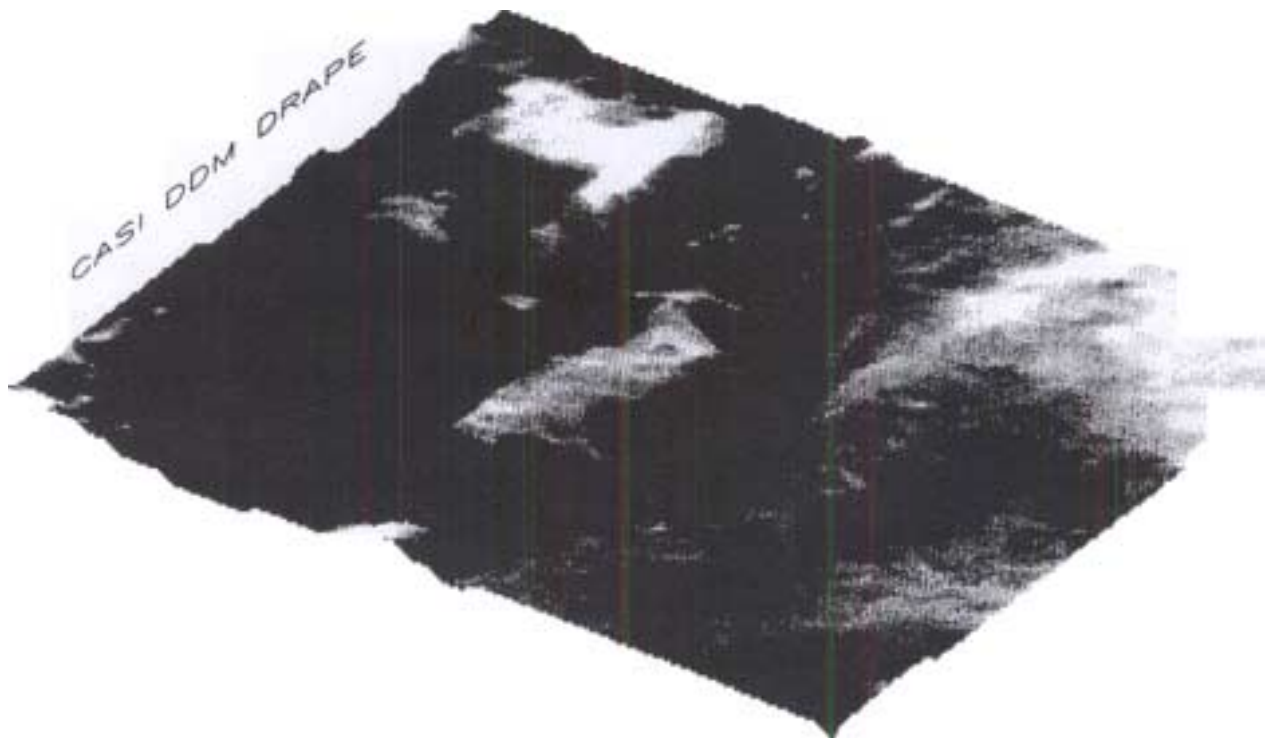


Figure 3 shows the same bottom area draped over a Digital Depth Model (DDM) of the sea bottom. This image display format is effective for giving an observer a feeling for the relative 'lay of the land', the bottom types present, and how they vary across the scene.

SUMMARY AND CONCLUSIONS

Steps for the preliminary production of bathymetric image maps using combined SHOALS LIDAR depth data and CASI hyperspectral imagery have been discussed. A listing of possible applicable algorithmic approaches for calculation of the water depth is outlined. Actual bathymetric image map information in two different image formats is provided.

The combined sensor system is seen to provide crucial information in the form of environmental spectral information, greater depth resolution, and water optics. It is this set of information which is necessary to begin to produce reliable remotely sensed bathymetric data. Moreover, as suggested above, such a data set allows for the unraveling of other environmental information such as bottom reflectance values -which leads to bottom type classification image maps.

ACKNOWLEDGEMENTS

Results and information presented, unless otherwise noted, are based on the work funded by Headquarters, U.S. Army Corps of Engineers, Operations, Construction, and Readiness Division and the Department of Industry, Science, and Technology, Canada. Permission to publish this paper was granted by the Chief of Engineers.

REFERENCES

- Billard, B. 1986. Remote sensing of the scattering coefficient for airborne laser hydrography. *App. Opt.*, 25, July.
- Borstad, G. and D. Hill. 1989. Using visible range imaging spectrometers to map ocean phenomena. *Proceedings of the Conference on Advanced Optical Instrumentation for Remote Sensing of the Earth's surface from Space, International Congress on Optical Science and Engineering, Paris, France, April 24-29, 1989.*
- Borstad, G. and J. Vosburg. 1993. Combined active and passive optical bathymetric mapping: using the Larsen LIDAR and the CASI imaging spectrometer. *Proceeding of the Canadian Symposium on Remote Sensing May 1993.*
- Estep, L. 1993. A suggested approach to the passive optical bathymetry problem by a component analysis of the upwelling remote sensing signal. *The Hydrographic Journal*, No.69, July 1993.
- Haimbach, So, Ho Mesick, Jo Byrnes, and D. Hickman. 1988. Optical Bathymetry for the US Navy. *Proceedings of SPIE Ocean Optics IX, Orlando, FL., April 1988.*
- Gordon, Ho 1982. Interpretation of airborne oceanic lidar: effects of multiple scattering. *App. Opt.*, 21' 16.
- Jerlov, N. 1976. *Marine Optics*, Elsevier, Amsterdam.
- Ji, W., D. Civco, and w. Kennard. 1992. Satellite Remote Bathymetry: A New Mechanism for Modeling. *PE&RS*, 58. Lillycrop, J. and J. Banic. 1992. Advancements in the US Army Corps of Engineers Hydrographic Survey Capabilities: The SHOALS System. *Marine Geodesy*, 15.
- Lyzenga, D. 1985. Shallow-water bathymetry using combined lidar and passive multispectral scanner data. *Int. Journ. Rem. Sens.*, 6.
- Philpot, W. 1987. Radiative Transfer in Stratified Waters: A Single- Scattering Approximation for Irradiance. *App. Opt.*, 26. Philpot, W. 1989. Bathymetric Image Mapping with Passive Multispectral Imagery. *App. Opt.* 28.